Nuclear Engineering and Design 307 (2016) 64–76

Nuclear Engineering and Design

journal homepage: www.elsevier.com/locate/nucengdes

Root cause study on hydrogen generation and explosion through radiation-induced electrolysis in the Fukushima Daiichi accident

Genn Saji [1]

Independent Research and Consulting, 4-39-3 Higiriyama, Konan-ku, Yokohama 233-0015, Japan

GRAPHICAL ABSTRACT

Unit	1F1	1F2	1F3	1F4 SFP
Photo : Courtesy of TEPCO				
	Mar.12, 2011	Apr. 10. 2011	Mar. 22, 2011	Mar. 22, 2011
Explosion	3/12, 15:38	~3/15, 06:14 (Note-1)	3/14, 11:01	3/15, 06:12 (Note-2)
Last DW Vent	3/12, 14:30	Note-3	3/13, 12:30	NA
Estimated H_2–m^3(STP)	29,400	86,200	58,800	700/d at 50 °C (best estimate value)

Note-1: At ~06:14, 3/15, an "explosive sound" was heard by the control room staffs. TEPCO's official view is no hydrogen explosion occurred in 1F2.
Note-2: The total fuel assemblies were stored in SFP (Spent Fuel Pool). The spent fuel was found intact.
Note-3: RPV depressurization through SRV at 3/15, 01:10. Suppression Chamber Pres. down-scaled to zero at 3/15, ~06:14 spontaneously. D/W pressure was 730 kPa(abs).

HIGHLIGHTS

- Reviewed how LWRs have coped with "water radiolysis", during normal operation to severe accidents.
- Concluded "water radiolysis" is not likely a route course of the hydrogen explosions at Fukushima.
- Performed modeling studies based on "radiation-induced electrolysis" on Unit 1–Unit 4.
- Generation of several tens of thousands cubic meters hydrogen gas is predicted before the hydrogen explosions.
- Upon SBO, early safe disposal of hydrogen from RPVs is indispensable in BWRs.

ARTICLE INFO

Article history:
Received 16 May 2015
Received in revised form 24 January 2016
Accepted 25 January 2016
Available online 15 July 2016

ABSTRACT

Since the scientific cause for a series of hydrogen explosions during the Fukushima accident has not been established, the author investigated his basic theory named "radiation-induced electrolysis (RIE)" by applying the estimation of the amounts of H_2 generation during the active phase of the Fukushima accident. The author's theory was originally developed by including Faraday's law of electrolysis into the basic time-dependent material balance equation of radiation-chemical species for his study on accelerated corrosion phenomena which is widely observed in aged plants. As such this theory applies to

E-mail address: sajig@bd5.so-net.ne.jp
[1] Ex-Secretariat of Nuclear Safety Commission of Japan (retired).

http://dx.doi.org/10.1016/j.nucengdes.2016.01.039

the early phase of the accident before the loss of water levels in the reactor cores, although the simulations were performed from the time of seismic reactor trip to the hydrogen explosions in this paper.
Through this mechanism as much as 29,400 m^3-STP of hydrogen gas is estimated to be accumulated inside the PCV just prior to the hydrogen explosion which occurred one day after the reactor trip in 1F1. With this large volume of hydrogen gas the explosion was a viable possibility upon the "venting" operation. In view of this observation, hydrogen generation from the spent fuel pools was also investigated.
For the investigation of the 1F4 SFP, the pool water temperature and flow velocity due to natural circulation were changed widely to identify conditions of large hydrogen generation. During the trial calculations it was discovered that SBO induced a rapid initiation of electrolysis when the pool water temperature surpassed 40 °C with a range of low water flow velocity through the spent fuels.
With a mix of different levels of radioactivity of spent fuel, a difference in the absorbed dose rate of water through γ-decay heat should have existed. This configuration induced an electrochemical potential difference between the highly radioactive region where there was spent fuel stored by evacuating the core and less radioactive fuels stored for several years. The spent fuel was stored in racks placed at the bottom of the pool where the wall was covered with a stainless steel lining. The metallic contacts enabled electric conduction between the highly radioactive fuel assemblies and the cooled spent fuel.

Nomenclature

BWR	boiling water reactor
CHC	critical hydrogen concentration
CVCS	chemical and volume control system
DH	dissolved hydrogen
ECCS	emergency core cooling system
ECP	electrochemical corrosion potential
HPCS	high-pressure core spray
IC	isolation condenser
LET	linear energy transfer
LWR	light water reactor
RPV	reactor pressure vessel
PCV	primary containment vessel
QSSA	quasi-steady state approximation
RHRS	residual heat removal system
RIE	radiation-induced electrolysis
SBO	station blackout (loss of all AC power sources)
SC	suppression chamber
SFP	spent fuel pool
SRV	safety and release valve

1. Introduction

A series of hydrogen explosions were undoubtedly the most dramatic events observed during the accident, however, its root-cause is one of the least known. Almost all of the investigation reports published by the National Government and Japanese Parliament as well as TEPCO's Investigation Committee explain the accident scenario as a tsunami-induced SBO which resulted in the core "melt-down" accidents (Nuclear Emergency Response Headquarters, 2011a, 2011b; National Diet of Japan, 2012; Investigation Committee, 2012; TEPCO, 2012). The resultant high temperature Zr-steam reaction generated a large amount of hydrogen gas, which leaked into the Reactor Building and then exploded.

TEPCO estimated amounts of hydrogen generation by employing severe accident analysis codes such as MELCOR, MAAP and SAMPSON. Unfortunately the predicted accident sequences and process data have not been validated with confidence due to the insufficient amount of reliable field data available during the active phase of the accident.

For example, in 1F1, total failure of Isolation Condenser (IC) and High Pressure Core Spray (HPCS) has to be assumed disabled due to the tsunami which arrived 51 min after the seismic reactor trip triggered on 14:46, March 11, 2011. However, the operators visually (i.e., by observing the ejection of steam from the exhaust pipe) confirmed that IC was judged working at 16:44, 18:18 and 21:30 on March 11 (TEPCO, 2012). The water level in RPV was barely showing at TAF (Top of Active Fuel) + 200 mm at 20:50 March 11 and TAF + 450 mm at 22:10 on the same day. This indicates that even HPCS, with its battery power, may have been working even after the arrival of the tsunami. With these objective observations, it is hard to believe the early melt-down scenario inducing hydrogen generation through Zr-steam reaction.

In spite of the widely accepted scenario, Prof. S. Murayama investigated this issue by developing a detailed time-dependent heat balance tool and concluded that "the IC was working after the tsunami arrival" (Maruyama, 2015). In addition to the discrepancy of theoretical simulations and objective field data, TEPCO has not been able to identify any evidence demonstrating the existence of corium (molten fuel debris) despite their investigation of the reactors inside the PCV as of 2015.

The most recent information directly related to the current status of the core is as follows. On March 19, 2015, TEPCO released their first snapshots of the cosmic-ray muon imaging detectors developed for 1F1. Although the resolution of this technology was only 1 m^2 due to the transmission method, the current data implies that no large fuel debris was left in the original core position, it is likely relocated below the core support plates (TEPCO's website, 2015a). Also on March 20, Nagoya University released an impressive report, which supports the core disintegration also in 1F2. They have been working on measuring muons since the spring of 2014, by using the muon particle detection system, which employs nuclear emulsion plate technology. This investigation focused on 1F2, where core melt is suspected due to the accident, and 1F5 where the fuels have been confirmed intact. The results revealed that the material mass in the 1F2 core region is 0–30% of the corresponding mass in 1F5 (Nagoya Univ., 2015).

Despite these muon imaging results TEPCO's recent robotic inspection inside the PCV of 1F1 identified only some sedimentation on the grating floor surrounding the lower portion of RPV (TEPCO's website, 2015b). This sedimentation is likely due to drooped anti-rusting paint (applied on the inner surface of PCV) molten due to an elevated temperature of only a few hundred centigrade but not consisting with the core melt-through event. It is difficult to explain the scenario of core melt followed with relocation to the PCV down to the PCV floor. Most of the core debris is likely still retained within the RPV. It is necessary to revisit the melt-through scenario which predicts the zirconium-steam reaction for the hydrogen generation by employing the severe accident analysis codes.

2. Water radiolysis in LWRs

In view of these conflicting reports the author will first review the water radiolysis phenomena which release hydrogen gas to elucidate how nuclear plants have been designed to cope with the effects of radiation on water. This is to look for some peculiar configuration which may have induced the hydrogen generation during the Fukushima accident. In general, water radiolysis has not been considered to produce a large amount of hydrogen in a short time.

The radiolysis of water is defined as a process of decomposition of water (H_2O) into di-oxygen (O_2) and di-hydrogen (H_2) due to ionizing radiation. The term water radiolysis is applied here as a narrower definition of the more general radiation-chemical reactions as defined as:

$$H_2O + \text{“radiation”} \rightarrow [e^-_{aq}, OH, H, HO_2/O_2^-, H_2, O_2, H_2O_2, H^+_{aq}, OH^-_{aq}] \quad (1)$$

When water is irradiated, it produces radical species (e.g., e^-_{aq}, OH, H and HO_2/O_2^-), stable ionic species (H^+_{aq} and OH^-_{aq}) as well as stable molecular products (e.g., H_2 O_2 and H_2O_2). Through complex chain reactions the final products are stable molecular products that are either in gaseous form or dissolved in water when their concentrations are low enough. The stable ionic species are seldom measured since they chemically interact with other ionic species contained in the reactor water.

2.1. PWR and critical hydrogen concentration

The Chalk River Laboratories (CRL) investigated the critical hydrogen concentration (CHC) required to suppress the net radiolytic production of oxygen and hydrogen. The CHC is the minimum concentration of dissolved hydrogen required to prevent the net radiolytic breakdown of water. Radiolysis is said to be suppressed when there is no net decomposition of the water with the addition of an excess hydrogen (Elliot and Bartels, 2009). This occurs when the concentration of oxygen and hydrogen peroxide are much lower than 1 μg/kg, i.e., $<-10^{-8}$ mol/kg.

It is worth noting that an excess of hydrogen is dosed in the primary coolant water of PWRs in order to prevent the accumulation of oxidant products (e.g., O_2 and H_2O_2) generally considered to be responsible for the corrosion of the primary system. The reactor water is purified by extracting a small portion of the primary water through CVCS, where hydrogen is purified and stored for recycling. However in practice, dissolved hydrogen will barely scavenge the radical species sufficiently before they convert much of the H_2O_2 back to water due to the short irradiation time in the core. It has also been shown that water decomposition by radiolysis in the presence of H_2 is a threshold phenomenon as a function of the LET of radiation (Caër, 2011). The reactivity control process with boric acid induces a significant alpha dose rate in PWR plants. In addition, recoil protons due to the scattering of fast neutrons induce track-averaged LET of several tens of eV/nm (Elliot and Bartels, 2009). It is likely that the water radiolysis is taking place in PWRs in spite of hydrogen dosing with the recoil proton and alpha irradiation.

2.2. Hydrogen generation and its processing in BWRs

The decomposition of water by radiation occurs even during normal operations in BWRs. In a Japanese licensing document (PSAR, Preliminary Safety Analysis Report) of a 1100 MWe BWR, the following description is given. “The waste gas extracted from the turbine condenser contains hydrogen gas and oxygen gas... They are diluted at the air ejector using steam ejection down to 4 vol%, which is below a hydrogen ignition concentration. Further, the hydrogen gas and oxygen gas are re-combined back to water and disposed finally by a gaseous waste disposal system.”

Although the water radiolysis in BWRs is a well-known phenomenon, its exact mechanism is not well defined, in the author’s opinion. It is likely due to a combination of the irradiation of boiling water, the un-closed configuration of the BWR plants and water chemistry without excess hydrogen dosing above CHC. In spite of these provisions there have been some incidences when the extraction of the hydrogen gas was not completely accomplished in the cooling system during normal operation. The hydrogen gas accumulated in air-pockets, such as located at the top vertical pipes and instrumentation piping, had exploded in several plants. This mechanism is important to understand the Fukushima accident, since a worker observed a rapidly increasing accumulated dose (0.8 mSv) as early as 21:31, March 11 while trying to enter the 1F1 Reactor Building. This observation is sometimes considered an evidence of a seismically induced pipe break or early core melt by some scientists.

In Germany, on 14 December 2001, a pipe break occurred inside the containment vessel of the Brunsbüttel BWR. The explosion took place in the so-called reactor core spray system area, which sprays cold water into the reactor vessel to cool down the reactor and remove residual heat in case of an emergency shutdown. When the reactor core spray system was inspected it revealed that a 10-cm diameter pipe had totally disintegrated over a length of 2–3 m. Although there is no clear explanation for the explosion it is suspected that a hydrogen explosion occurred (Brunsbüttel reactor, 2002).

Prior to this accident a pipe burst occurred in Japan’s Hamaoka-1 BWR on November 7, 2001 (Nuclear and Industrial Safety Agency, 2002; Naito et al., 2003a,b). When the HPCS was started up for a routine test operation, a pipe ruptured and radioactive effluent was released into the reactor building. The reactor was in a normal state of power operation. A brief outline of this accident is summarized in Appendix A. It was later disclosed that there were 8 other incidents linked to hydrogen explosions that have been experienced inside TEPCO’s instrumentation and control systems at several BWR plants, where air pockets or stagnant water/gas separation was likely (TEPCO website, 2003, in Japanese).

It remains a mystery how the hydrogen- and oxygen gases are generated and separated from the water in the HPCS, accumulated in an air pocket and then ignited. The hydrogen generation through water radiolysis has been well known however, how the presence of oxygen in stoichiometric amount indicates a potential involvement of radiolysis. This mode of “internal” hydrogen explosion may have occurred in 1F1 at around 21:51, March 11 since TEPCO’s crew detected high dose rate inside the reactor building. Due to SBO the forced water circulation was not available which should have facilitated separation of hydrogen and oxygen gas from the water at a air pocket.

2.3. Water radiolysis in open/closed systems

Irradiation of pure water in a closed system by low-LET radiation leads to the establishment of a steady state in which low concentrations of hydrogen, oxygen and hydrogen peroxide are present (Spinks and Woods, 1990). However, under certain conditions hydrogen gas is released from the water under irradiation. Sophie Le Caër reviewed the mechanisms accounting for the radiolysis of water with an emphasis on H_2 production and the modifications of H_2 production in radiolysis at water/oxide interface (Caër, 2011).

According to the textbook, “irradiation of pure water in a system that is not closed leads to buildup of a steady-state concentration of hydrogen peroxide in solution and the continual escape of hydrogen and oxygen from the system; in effect, the radiation

decomposes the water into hydrogen and oxygen." This configuration represents the BWR's reactor water inside the RPV. However the author was unsuccessful in confirming this phenomenon through radiation chemical calculations. It released oxygen instead of hydrogen in a trial calculation. The actual behavior is much complicated as demonstrated in the following chapters.

2.4. Scoping estimation of water radiolysis for the Fukushima accident

The author has published a scoping estimation of the hydrogen generation through water radiolysis without considering the radiation-chemical chain reactions (Saji, 2014a). The accumulated volumes of hydrogen gas until the hydrogen explosions were 450/1100/900 m^3-STP for 1F1/1F2/1F3, respectively. By considering the reverse chain reactions, the volumes of hydrogen gas were much less than 100 m^3-STP, an order of magnitude less than the estimation made simply by using *G*-values. Through this estimation it was concluded that the water radiolysis should not be the root cause for the series of hydrogen explosions (Saji, 2014a,b).

2.5. Hydrogen release and explosion during the Fukushima Daiichi accident

In the Fukushima Daiichi BWR plants the radiolytic hydrogen was generated through gamma radiation from the fuel inside the RPV but it appears not to have been retained within the reactor water. The dissolved hydrogen gas was separated inside the RPV of the BWR, since the top half of RPV was filled with steam while the reactor water was at the bottom half. Upon the termination of the decay heat removal systems the RPV pressure soon increased above the set points of the SRVs due to the boiling and started to release steam to the suppression pool. The safety valve function was mechanical and automatically released the overpressure into the Suppression Chamber (SC) of the PCV even with SBO. It also should have released hydrogen gas into the SC which eventually spread to the entire PCV.

To cope with potential generation of hydrogen gas in an event of design basis LOCA the Fukushima Daiichi plants had Standby Gas Treatment Systems (SGTS). The hydrogen gas generated through the zirconium-steam reaction should have first been re-combined prior to release. An emergency electrical power source was necessary for the operation of the SGTS; but it was not available due to the SBO. Without this system hydrogen gas generated through water radiolysis kept accumulating inside the PCV. Upon venting of the PCV the hydrogen gas back-flowed into the Reactor Building through ventilation ducts which triggered the hydrogen explosion.

3. "Radiation-induced electrolysis" (RIE)

The review of water radiolysis as summarized in Chapter 2 generally concludes that the "water radiolysis" is unlikely the root cause of the large amount of hydrogen generation which occurred during the Fukushima Daiichi accident. With this notion, the author investigated the applicability of his basic theory entitled "radiation-induced electrolysis (RIE)" for the estimation of the amounts of H_2 generation during the active phase of the Fukushima accident.

The RIE is induced in metallic components through which the conduction-electrons flow to the cathodic region whose redox potential is elevated due to radiation. This mechanism is different from "radiolysis" which is the dissociation of molecules through the direct exposure of nuclear radiation.

The author's theory was originally developed by including Faraday's law of electrolysis into the basic time-dependent material balance equation of radiation-chemical species for his study on accelerated corrosion phenomena widely observed in aged plants. As such this theory applies to the early phase of the accident before the loss of water levels in the reactor cores, although simulations were performed from the time of seismic reactor trip to the time of hydrogen explosions in this paper.

3.1. Evidence of RIE

The RIE hypothesis was proposed based on experimental observations demonstrating the electrical potential differences between the irradiated and the non-irradiated regions of the water contained in the metallic loops modeling LWRs. The potential difference should have induced electrolysis resulting in the decomposition of water into hydrogen and oxygen.

For the BWR water chemistry sphere there are several experimental evidence demonstrating that irradiation can induce potential differences between the irradiated and un-irradiated regions, which is an interesting mechanism specific to the nuclear reactor environment. Although this effect is well established through many independent experiments which have been assessed by the author (Saji, 2010a), there are very few "controlled" experiments which are robust enough to withstand further theoretical studies. When there exists a potential difference, there should be various RIE phenomena[2] driven by the electrical current.

More recently redox potential differences were published for BWR-NWC (Kysela et al., 2001; Zmikto, 2003) as well as for PWR (Takiguchi et al., 2000, 2004). These report demonstrated the existence of +0.1(BWR-NWC) to +0.3(PWR) V ECP differences between the in-flux ECP electrode and those at the out-of-flux regions. The author has been trying to theoretically reconstruct these experimental evidences by integrating Faraday's law of electrolysis into the radiation chemical material balance equation (Saji, 2016a,b). At this stage it is still necessary to confirm or determine the weight of the radiation-induced perturbation to the Nernst equation by introducing the "conductive-dielectric correction." The qualitative discussion supports the reason why this correction factor is as large as 11.6 for BWR-NWC while it is 1.0 for PWR when the proton hopping model is incorporated in the latter. In spite of these reservations, the author's initial objective is now basically completed by establishing the RIE as the root cause for the peculiar corrosion phenomena being experienced in aged LWRs.

The demonstration of the applicability of the RIE mechanism in the corrosion study is rather complicated, since it is necessary to convert the concentrations of radiation chemical species into the potentiometric unit of electromotive force (i.e., volt). The concentration of radiation chemical species were obtained by applying the "improved" QSSA method which provides solutions through the Lagrangean formalism, although the Eularian time integration method is more widely applied in the radiation chemistry arena. The applicability of the improved" QSSA is somewhat controversial. Further details will be discussed in Section 3.4.

However, the estimation of the amount of hydrogen generation in the event of a severe accident is more straightforward since it is calculated directly from the radiation chemical material balance equation. The only new idea is in the incorporation of Faraday's law on electrolysis in the radiation chemical material balance equation. This approach is motivated from the review of the basic corrosion hypothesis as summarized in the author's conference paper (Saji, 2015, 2016a,b).

[2] The word "electrolysis" is used in this report to imply that both hydrogen- and oxygen gases may be generated sometimes in an stoichiometric amount, in contrast to another mechanism of "water radiolysis" which occurs in non-metallic systems.

3.2. Mechanism of RIE

The observed potential difference was measured through in-pile tests with an equivalent hydrogen standard electrode which is formulated by dosing the primary water with hydrogen gas in PWRs and a standard electrode that is inserted in the flux region.[3] In the measurement, the potential of the electrode was raised by 0.1(BWR-NWC)–0.3(PWR) V by applying an external battery to cope with the redox potential. Note that the hydrated electrons, with their short lifetime, do not flow directly to the electrode but rather they raised the redox potential of the water and induce electrochemical electron current from the cathodic metallic wall to the water, as in the case of electrical batteries through:

$$2H^+ + 2e^-_{\text{cathode}} \rightarrow H_2 \tag{2}$$

Generation of hydrogen through Eq. (2) may not result in an increase of the hydrogen concentration at the core region due to the fact that the concentration is determined by an overall radiation chemical material balance combined with the in-core dose rate. In the situation of in-core concentrations that are higher than the out-of-core region, hydrogen is reverted back to hydrogen ion at the out-of-core region through oxidation of hydrogen:

$$H_2 \rightarrow 2H^+ + 2e^-_{\text{cathode}} \tag{3}$$

Here the excess e^-_{cathode} is transported back to the cathodic reactor core region through piping thereby closing the electron conducting circuit. Should this mechanism be absent, such a system will shift to the state of water radiolysis in an open configuration in the BWR whereas in the PWR, due to its closed configuration, the system will lead to the establishment of an autonomous steady state as described in Section 2.3. With such a configuration the hydrogen or oxygen concentration should become uncontrollable contrary to the in-pile tests where these concentrations are adjusted for water chemistry control.

The set of electrochemical reactions between the in-core and out-of-core regions results in a net effect of conduction electrons (i.e., long-cell current) flowing from the cathodic surface (e.g., fuel cladding) into the redox water. The hydrated electrons release their energy into the redox water contributing to the higher potential. The (more positive) higher potential with the redox water repels the positive charged ions (e.g., H^+) toward the metallic walls to react with cathodic electrons when the reactor water is conductive with solute ions as in the case of the PWR water chemistry. When the conductivity is small as in the case of BWR-NWC, the dielectric property should be identified.

This simplified interpretation is important to understand the role of other radical reactions without a charge transfer, consisting of the reaction of a "reductive" H radical, and an "oxidizing" OH radical and a stable molecular product H_2O_2. The author's radiation chemical calculation includes the overall material balance of these species in computing the concentration of oxidized species such as hydrogen $[H_2]$ and $[O_2]$ in the primary water; however radical reactions are not included in the charge transfer process at the electrode.

The author has shown that such a potential difference is induced through the annihilation of hydrated electrons (e^-_{aq}) generated under radiation (Saji, 2010a,b, 2013a,b). However e^-_{aq}, with their short lifetime, do not flow directly to the electrode. Rather the hydrated electrons generated in the core region participate in raising the redox potential of the water and induce an electron current from the metallic wall to the water, as in the case of electrical batteries.

[3] For simplicity purposes, the hydrogen polarization case is discussed here since our interest is on hydrogen generation.

3.3. Electrolytic generation of hydrogen and oxygen

The most common electrochemical charge transfer reactions occurring on the surface of the electrodes for LWRs include;

$$2H^+ + 2e^-_{\text{cathode}} = H_2 \tag{4}$$

$$O_2(aq) + 4H^+ + 4e^-_{\text{cathode}} = 2H_2O \tag{5}$$

$$H_2O_2 + 2H^+ + 2e^-_{\text{cathode}} = 2H_2O \quad \text{and} \tag{6}$$

$$O_2 + 2H^+ + 2e^-_{\text{cathode}} = H_2O_2 \tag{7}$$

These reactions can be generally expressed as:

$$Ox + ne^-_{cathode} \leftrightarrow Rx \tag{8}$$

where Ox is the oxidized- and Rx is the reduced species and n is the electric charge transferred through the particular reaction involved. These reactions provide electrodes on the surface of metal when e^-_{cathode} is removed by the equilibrium electrochemical potential, E_o, of the irradiated water.

Note that Eq. (4) represents the dominant electrochemical reaction in the PWR water chemistry environment, whereas Eqs. (3)–(5) are major reactions in the case of BWRs. As a matter of fact, the author's theoretical study on the NRI-Rez's in-pile test results revealed that the out-of-flux potential was expressed by Eq. (5) + 0.396 Eq. (7), whose potential is upshifted due to the residual hydrogen peroxide in the out-of-flux region (Saji, 2016a).

3.4. Theory of RIE

Since detailed development and verification have already been published (Saji, 2010a, 2013a,b, Saji, 2014c, 2016a,b), only the essential portion is presented in this section. The basic time dependent material balance equation for Ox in the radiation chemical environment can be described in Eq. (9), when the electrochemical processes (i.e., Faraday's law) are included in a "point model" (where the flux region is lumped together into a single water volume V_o), as:

$$\frac{dC_{Ox}}{dt} = \{G(Ox)\dot{D} + \sum_{qr} k^{Ox}_{qr} C_q C_r + \dot{\nu} C^{in}_{Ox}\} - C_{Ox}\{\sum_{s} k_{Ox,s} C_s + \dot{\nu}\} + \frac{A_o i_{cathode}}{nFV_o} \tag{9}$$

where C_i is the concentration expressed in mol/dm^3 for species X_i, $G(Ox)$, the G-value in mol/J for species Ox $\dot{D}$ is the absorbed dose rate of water in J/dm^3, k_{is} is the rate constant between species X_i and X_s in dm^3 mol^{-1} s^{-1}. The rate constants k^i_{qr} (represented for the second order reactions) between species X_q and X_r, have non-zero values only when the reactant species is X_i, in dm^3 mol^{-1} s^{-1}. The 'normalized' volumetric flow rate $\dot{\nu}$ represents the flow rate (1/s) of the coolant in the active region within a point model and C^{in}_{ox} is the concentration of the Ox in the incoming flow, which applies to the stable molecular species[4] such as H_2, O_2 and H_2O_2.

Note that the third term provides the corresponding incoming or removing flux of species Ox due to electrolysis at the metallic surface through Faraday's law. As such a numerical simulation, $(dC_{Ox}/dt)_{electrolysis}$ was calculated without decomposing the third term into the electrolysis parameters consisting of the cathode current $i_{cathode}$, the Faraday constant F and the total surface area of the cathode A_o. In the simulation, the net flux of Ox due to the

[4] The incoming flow of hydrogen ions $[H^+]$ and hydroxyl anions $[OH^-]$ should also be included in this formalism in principle however; the deviation is small due to Ostwald's law except at the lower ends of the DH and DO concentrations.

Table 1
Operational history of Daiichi.

	Unit 1	Unit 2	Unit 3
P_o	1380 MWt	2381 MWt	2381 MWt
$\tau_{elapsed}$	1–24 h (variable)	1–155.2 h (variable)	1–70 h (variable)
τ_s	1.46E+07 s (169 d).	9.763E+06 s (113d).	9.763E+06 s (113 d)
Explosion	15:36, March 12, 2011	06:14, March 15, 2011	11:01, March 14, 2011

RIE is determined to maintain the material balance of the radiation chemical configuration under investigation.

In the steady state, Eq. (9) is simplified to Eq. (10):

$$C_{Ox} = \frac{G(Ox)\dot{D} + \sum_{qr} k_{qr}^{Ox} C_q C_r + \dot{v} C_{Ox}^{in} + A_o i_{cathode}/nFV_o}{\sum_s k_s^{Ox} + \dot{v}} \quad (10)$$

In the last term of Eq. (9), representing the electrolytic generation/removal of *Ox*, the sign of $i_{cathode}$ is assigned as positive current for the forward reaction (reaction to the right) in Eq. (8). It is important to point out that the cathode current can be introduced through external systems coupled with the water chemistry configuration outside of the radiation chemical system under consideration in the point model.

Whereas the concentrations of the short-lived radical species are calculated by Eq. (11):

$$C_i = \{G(X_i)\dot{D} + \sum_{qr} k_{qr}^{i} C_q C_r\} / \{\sum_s k_{is}^{i} C_s\} \quad (11)$$

The simplification with a set of Eqs. (10) and (11) is called "improved" QSSA in which the concentrations of radical species, Eq. (11), jump promptly to the new concentrations due to their short time constants. It is widely used for the integration of "stiff" ordinary differential equations[5] arising from the photolysis effects in the atmospheric chemistry arena (Jay et al., 1995). When the equation dealing with long-lived molecular species is not separated from the equation for short-lived radical species such simplification is called the "plain" (i.e., original) QSSA.[6] The latter may not result in appropriate solutions as discussed by Farrow and Edelson (1974).

For further quantitative discussions, it became increasingly important to use the established radiation- and electro-chemistry data sets in order to proceed any further. Dr. A.J. Elliot of AECL and Prof. S.M. Bartels of Notre Dame Radiation Laboratory (hereafter called "E-B data") released a new set of data in 2009 (Elliot and Bartels, 2009). The author has incorporated this information to verify previous calculations published in earlier papers.

In solving the set of equations in the improved QSSA, it was necessary to calculate the change in dose rate due to decreasing decay heat in 1F2–1F3 (under the constant temperature) or the increasing pool water temperature in 1E4 (with constant dose rate). These data were calculated by using the functional representation of radiation chemical data set as provided in the reference (Elliot and Bartels, 2009). These variation were incorporated in finite difference representation of the radiation chemical material balance equations.

[5] In mathematics, a stiff equation is a differential equation for which certain numerical methods for solving the equation are unstable, unless the step size is taken to be extremely small.

[6] The "improved" QSSA is more useful for practical engineering applications, since it is formulated in the Lagrangean coordinate, although the time-integration scheme in Eulerian co-ordinate is more widely used among radiation chemists.

3.5. Modeling study of hydrogen generation in 1F1–1F3

(1) In-vessel natural circulation should occur through the jet pumps. Dissolved hydrogen is mixed and diluted with large volume of reactor water in the upper and lower plenums before flowing to the core region.
(2) The reactor core region is cathodic due to radiation, whereas out-of-core region is anodic in the reactor water, comprising a "differential radiation cell".
(3) The electrons generated at the surface of the anodic out-of-core components are transported to the fuel rods. These components are in direct metallic contact facilitating the flow of electrons.
(4) Excess hydrogen is released from the core region. Over pressure due to boiling is released together with hydrogen through SRV to the suppression pool, eventually diffused inside of the PCV.

3.5.1. Decay heat and plant parameters

The following empirical equation accounts for both gamma as well as beta energy releases in the decay heat estimation (McMaster Nuclear Reactor, 1998).

(1) $P/P_o(\beta+\gamma) = 0.066[\tau_{elapsed}{}^{-0.2} - (\tau_s - \tau_{elapsed})^{-0.2}]$, where $\tau_{elapsed}$ is the time that elapsed after the reactor shutdown, τ_s is the time of the reactor startup.
(2) $P/P_o(\beta) = 0.031[\tau_{elapsed}{}^{-0.2} - (\tau_s - \tau_{elapsed})^{-0.2}]$.
(3) Operational history (Table 1).
(4) Plant parameters (Table 2).

3.5.2. Radiation-chemical data

The radiation-chemical analysis uses data developed by AECL's A.J. Elliot and D.M. Bartels.

(5) g(H_2)-value

0.62 per 100 eV at 290 °C = 0.10364 × 0.62 (mM/J)

Note that this is the primary yield and does not provide the concentration of hydrogen after going through a chain of radical reactions.
(6) Rate constant dataRate constant data were calculated from the functional representation as provided in Reference (Elliot and Bartels, 2009) as performed in the author's corrosion studies.
(7) Equilibria and associated rate constants of H_2OA change in the pH and concentration of water (in mol/L) with respect to the temperature was calculated from the polynomial representation of pK_{H_2O} provided in reference (Elliot and Bartels, 2009).
(8) Radiation chemical calculationA series of radiation chemical calculations were performed by applying the "improved QSSA".

3.5.3. Results of estimation of H_2 generation

The plant data assumed in the following modeling study are summarized in Tables 1–3. The "mixing water volume" listed in Table 2, is the volume of water in which the fuel assemblies are submerged, typically the total water hold-up in RPVs or SFPs. The mixing effect dilutes the DH concentration of the irradiated water before it recycled back to the entrance of the fuel assemblies. This

Table 2
Plant parameters for scoping estimation.

	Unit 1	Units 2–3	Unit 4
Total thermal power (MWt)	1380	2381	1.95 (note 1)
Effective core dia (m)	3.439	4.03	–
Irradiated H_2O inventory (m^3)	22.8	27.7	166 (SPF) (note 1)
Mixing water volume (m^3)	200 (RPV)	300 (RPV)	1425 (SFP)
Water temp (°C)	290	290	20–100 (parameter)

Note: The following sets were also tested: 1.95 MW_t/166 m^3; 1.95 MW_t/50 m^3; 1.83 MW_t/80.7 m^3. The last set represents the dominant decay heat from the last 24th and the last to one 23rd fuel cycles.

Table 3
Scoping estimation of accumulated hydrogen gas in PCV until the H_2 explosion.

	Unit 1	Unit 2	Unit 3
H_2–m^3 (STP)	29,400	86,200	58,800
Explosion	15:36, March 12, 2011	06:14, March 15, 2011	11:01, March 14, 2011
Elapsed time	24.1 h	155.2 h	68.2 h

process was found to significantly reduce the suppression of the hydrogen generation rate retarding the saturation with DH. As such, the current estimation is much larger than those estimated in the author's previous publications (Saji, 2014a,b).

For numerical calculation a simple EXCEL® program was developed to solve 8 (columns) × 37 (including 13 buffer memory lines) matrix through a relaxation technique for 1F4 SFP. For 1F1–1F3, the matrix consists of 39 columns (with 13 buffer memory columns) and up to 50 lines of time segments to account for the time dependency of the decay heat. The results illustrated in Figs. 2–4 as well as those summarized in Table 3 should be regarded as the consultation values when water radiolysis is assumed to have occurred through the RIE mechanism.

These values were made through various modeling studies which revealed the involvement of the following uncertainties:

(1) The estimated values can be smaller than the actual ones since the release (i.e., removal) of hydrogen gas through SRV into the PCV is not considered. This assumption increases the DH concentration in the reactor water resulting in an effect of over suppression of the RIE process.
(2) The estimated values may be smaller since the water level inside the RPV is assumed as being unchanged until the initiation of the hydrogen explosion. When decay heat removal through HPCS, IC or RCIC became unavailable, the steam release through SRVs induced a gradual decrease in the water level.
(3) Uncertainties induced by the residence time, which is the average time the water molecule should stay in the active part of the fuel, and the duration of the reactor water flowing through the active region of the core, are assumed by the author's engineering judgment. It may have changed largely during the course of the accident through decreasing decay heat, channel boiling and the natural convection effect of the irradiated reactor water. Fortunately this effect is not substantial as shown in Figs. 1–3 where the gradual accumulation of hydrogen gas with time is shown for the residence time of 10 s and 100 s.
(4) Mixing, dilution and the recirculation effects of water. The author assumed it is proportional to the volume of irradiated water and the reactor water involved in the in-vessel natural circulation process.

In spite of these uncertainties, it is safe to say that the initial root cause of the hydrogen generation with the SBO is through RIE, which occurred before the onset of the zirconium-steam reaction. The latter reaction may have aggravated the Fukushima Daiichi's accident situation.

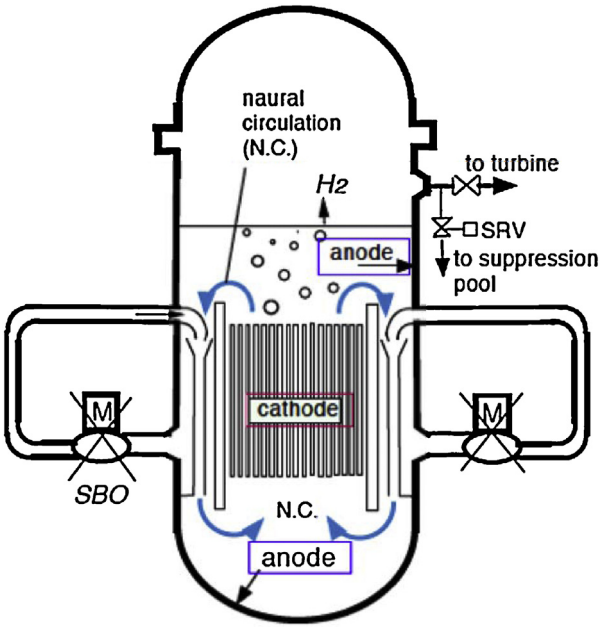

Fig. 1. Configuration of Fukushima Daiichi Unit 1–3.

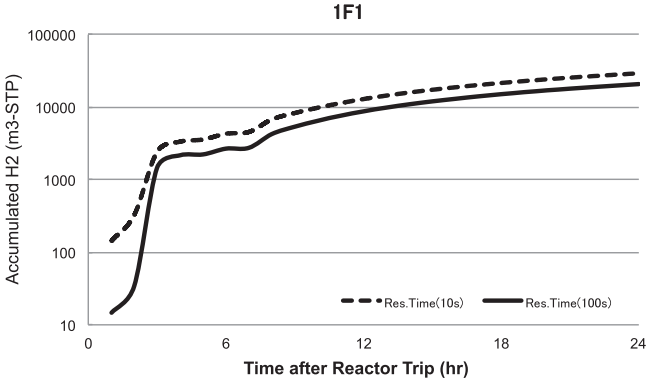

Fig. 2. Accumulated H_2 in Unit 1 (m^3-STP).

4. H_2 generation in the spent fuel pool of 1F4

TEPCO's official view is in line with the hypothesis that the hydrogen gas generated through the core-melt accident in the adjacent 1F3 leaked into 1F4 through the shared ventilation duct. The

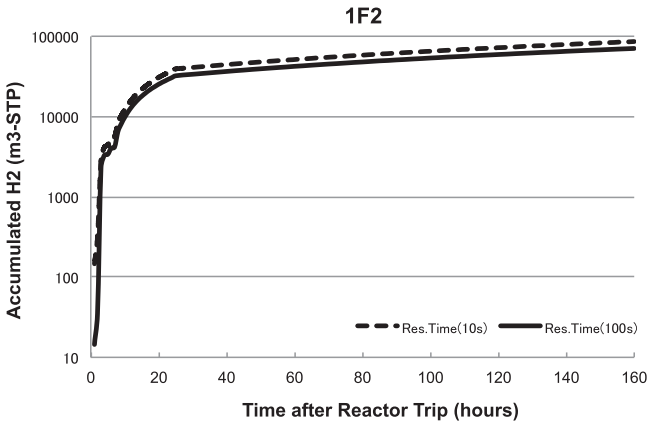

Fig. 3. Accumulated H_2 in Unit 2 (m^3-STP).

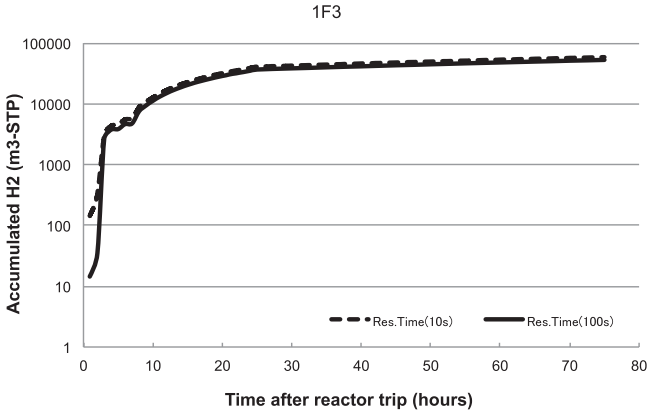

Fig. 4. Accumulated H_2 in Unit 3 (m^3-STP).

overpressure in the 1F3 reactor containment vessel was vented through an inverse Y (i.e., Ψ) shaped pipe joint located at the bottom of the shared stack, which was shared between 1F3 and 1F4. Each of the two legs of the pipe joint were connected to the vent lines from 1F3 and 1F4. TEPCO's explanation is hard to believe since the high speed gas vented from 1F3 was more likely extracted the air from the 1F4 rooms at the pipe joint as in the case of a spraying nozzle. In addition the hydrogen explosion in 1F4 SFP occurred 35.6 h after the last venting operation in 1F3, where the hydrogen explosion occurred at 11.01 of March 14th.

The basis of TEPCO's argument is in the observed higher concentration of radioactive cesium deposited on 1F4's ventilation filter banks at their exhaust side rather than those of the inlet banks. TEPCO's emergency team also noticed a high dosimeter reading (8 mSv) at 9 am of March 13th. They gave up entering the 1F4 Reactor Building due to the high dose. The flow reversal may have occurred at the time of the hydrogen explosion in 1F3 which erupted at 11:01 on March 14th, however, TEPCO's observation does not prove that the vented hydrogen from 1F3 flowed continuously into 1F4. Therefore the possibility of hydrogen generation through RIE in 1F4 should also be investigated.

4.1. Modeling of hydrogen gas generation in SFPs

The hydrogen generation rate was calculated by applying the author's theory as explained in Sections 3.3 and 3.4 with adaptations to the SFP configuration which includes decay heat, spent fuel management as well as the placing of spent fuel racks in the pool. Fig. 5 illustrates a RIE model for the case when a region of the SFP was cleared to store the evacuated core (i.e., 24th core loading) in

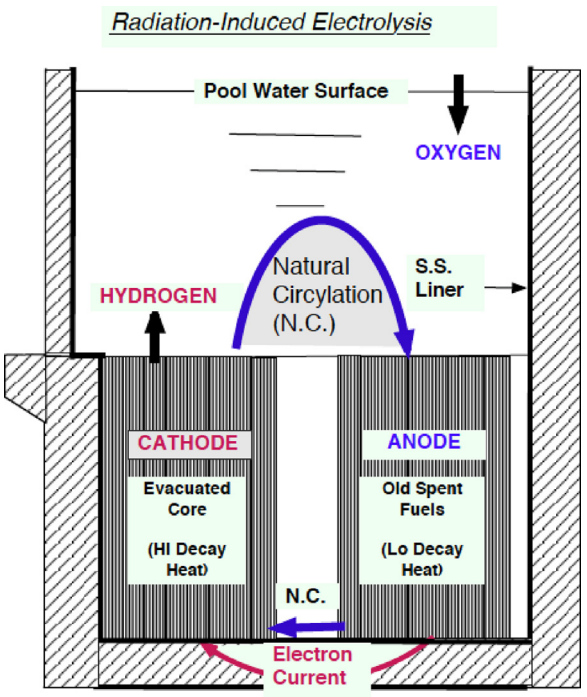

Fig. 5. Radiation-induced electrolysis in 1F4 SFP.

the left hand side zone as shown in Fig. 5 by moving the fuel bundles from the previous 6 cycles to another side.

In Fig. 5, the natural circulation flow route, conduction electro flow route as well as anodic and cathodic region are also illustrated. Note that the electrons are flowing from the anodic region (fuel bundles from the previous 6 cycles) to the cathodic region (evacuated core) where the absorbed gamma dose rate in the pool water was higher than the previous 6 cycles.

4.1.1. Operational cycles and spent fuel management

The new estimation begins with a more precise estimation of the decay heat in 1F1 through 1F4 by tracing past re-fueling history to the oldest spent fuels stored in the SFPs. Since re-fueling operations are performed for ¼ of the total core loading at a cycle, it was necessary to follow the refueling records for the last 4–5 re-fueling cycles which covers a time span of 6–10 years. The total number of fuel assemblies moved to the SFP which were calculated from the operational records is consistent with TEPCO's recent inventory data of the total spent fuel stored at the time of the accident (TEPCO's website, 2014) except for several fuel assemblies likely stored in special containers which are provided for leaking or bent fuel bundles.

The 1F4 SFP had a storage capacity of 1590 fuel assemblies. The most recent (24th) fuel cycle was completed on November 30, 2010 and the entire core loading of 548 fuel bundles were transported to the SFP by shuffling the existing 685 spent fuel bundles exchanged during the previous 6 cycles. However, it is not clear whether these hot fuel assemblies were rearranged among the previously stored spent fuel, which have a lower decay heat, or whether a region was cleared to store the entire 24th core loading in one region by moving the fuel bundles from the previous cycles. This uncertainty results in a large variation in the estimated amount of hydrogen generation due to the change in absorbed γ-dose rate and the total volume of highly irradiated water.

(1) Natural circulation between the evacuated core and old spent fuels from past fuel exchange operations. Fuel assemblies were

Table 4
Estimated total decay heat (on 3/11 2011).

Units	SFP water (m^3)	DH (MW_{total})	Water injection
1F1	1220	7.51E−02	2011/3/31∼
1F2	1425	4.45E−01	2011/3/20∼
1F3	1425	4.13E−01	2011/3/17∼
1F4	1425	1.95E+00	2011/3/20∼

stored in spent fuel racks which allow water circulation from the bottom through fuel assemblies.
(2) The evacuated core is more cathodic due to higher decay heat than the historical fuel assemblies.
(3) Electron current should be flowing from the historical fuels → spent fuel racks → stainless steel liner → spent fuel racks for the evacuated core → cathodic evacuated core.
(4) Excess hydrogen should be released from the evacuated core when the dissolved hydrogen exceed the solubility limit determined by Henry's law.

4.1.2. Decay heat

Table 4 summarizes decay heat of spent fuels stored in SFPs estimated by applying the equations as per Section 3.5.1 to adapt the operational history of spent fuel as summarized in the previous section.

It is reasonable to focus on the situation at 1F4 in view of the fact that the decay heat emitting from this SFP was approximately 4 times larger compared to 1F2 and 1F3. If the accident is assumed to have initiated one month after the last shutdown (i.e., December 30, 2011) in 1F4, then the decay heat was 3.55 MW. This case will also be investigated in the follow-up calculation to clarify the safety margin.

The estimated 1F4 decay heat value can be verified by using an actual measurement (TEPCO's website, 2014), with the reported pool water temperature of 84 °C at 4:08 on March 14th, 61.2 h after the earthquake. The time span to reach this temperature is 53 h (13% error) in the author's estimation when the initial pool water temperature was assumed to be 25 °C. Note that the pool water temperature was increasing in an order of 10 °C per day. Since the empirical results are within errors of the order of +10% and −20% of the ANS Standard (ANS-5.1, 1973), which likely contains some safety margins, the results can be judged close to the actual value of 1F4. A part of the deviation should also be due to convection heat dissipation from the pool water.

4.1.3. Cooling of spent fuel in the pool

During the accident the spent fuel cooling should have been accomplished through a single-phase natural circulation or sub-cooled boiling when the pool water temperature approached near the boiling point. Since the boiling heat transfer removes the decay heat very effectively, as such the overall mass flow rate should have decreased substantially.

4.1.3.1. Natural circulation modeling. Several videos taken on top of the 1F4 pool during the accident were showing that the pool water surface seems to be tranquil above the spent fuel racks when the pool water temperature is below approximately 80 °C. Above this temperature, noticeable "ripples," as well as steam bubbles, were identified. This observation may indicate either the occurrence of local boiling or a release of hydrogen gas. In the following study, both a single-phase case as well as a two-phase natural circulation case are modeled.

In the single-phase natural circulation heat transfer, the pool water enters from the bottom of the fuel, rising inside of the fuel assembly and then outflows into the bulk of pool water at 100 °C. This assumption should provide a lower dissolved hydrogen gas transport from the active region. The residence time, which is the average time that the water molecule should stay in the active part of the spent fuel, is calculated through the heat balance necessary to remove the decay heat. Results are shown in Fig. 6.

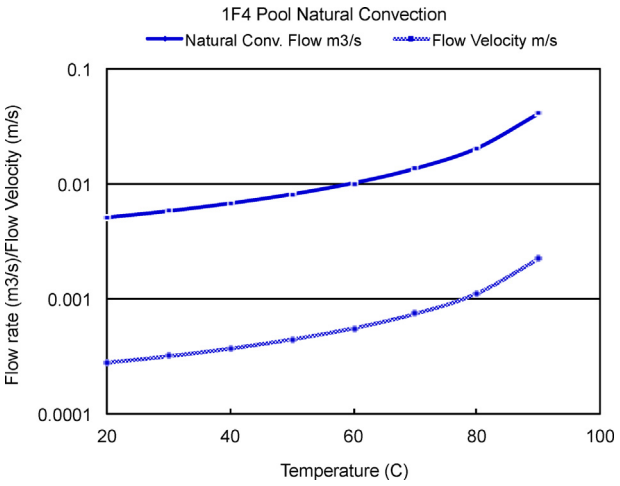

Fig. 6. Total flow rate and flow velocity through evacuated fuel assemblies in 1F4 spent fuel pool.

Table 5
Solubility of H_2 and initial DO (mol/m^3) at 1F4 Pool.

Temp. (°C)	Ca (H_2)	Ca (O_2)
20	7.80E−01	2.72E−01
30	7.37E−01	2.30E−01
40	7.00E−01	1.96E−01
50	6.66E−01	1.69E−01
60	6.36E−01	1.47E−01
70	6.08E−01	1.29E−01
80	5.84E−01	1.14E−01
90	5.61E−01	1.02E−01

In the two-phase natural circulation modeling, it was assumed that sub-cooled boiling initiated at above 80 °C. Below this temperature the single-phase natural circulation was it was assumed to be dominant. With the initiation of the sub-cooled boiling, the flow velocity was assumed to have decreased sharply (approximately 6×10^{-5} m/s) due to its excellent heat transfer due to its high evaporation heat.

4.1.3.2. Henry's law (Sander, 1999). The SFP will not be able to retain a DH higher than the solubility limit of hydrogen. The excess DH concentration above the saturation concentration calculated with Henry's law can be applied to calculate hydrogen release rates.

(1) Dissolved hydrogen
It is assumed that the maximum pressure at the active water zone is 2.2 atm. abs. (12 m from the pool water surface).
(2) Dissolved O_2
The dissolved oxygen concentration for the in-flow of the water to the spent fuel was calculated through Henry's law with the partial pressure of 0.20946 atm. This is to assume that the bulk of the pool water is saturated with oxygen at its surface (Table 5).

4.1.3.3. Temperature dependence of the reaction rate set. The sudden initiation of hydrogen releases as predicted in previous reports (Saji, 2014a,b) is puzzling. This phenomenon appears to occur through the RIE due to a breakdown of the radiation chemical configuration of the water chemistry at 40 °C in 1F4. The cause was

traced back to the strong temperature dependence of the spontaneous decomposition of H radical:

$$H \rightarrow H^{+} + e^{-}_{aq} \quad (12)$$

whose reaction rate changes nearly three orders of magnitude between 20–100 °C (i.e., 3.70E+00 → 1.31E+03, respectively) according to the reference (Elliot and Bartels, 2009). Obviously, further in-depth study on the predicted behavior of hydrogen release is necessary.

4.2. Estimation of hydrogen generation

4.2.1. Configuration of spent fuel in 1F4

The author realized the following uncertainties for further quantitative discussion.

(1) Management of spent fuels for the core evacuation
The radiation calculation starts with *G*-values (i.e., μmol/J) which depends on the radiation chemical yield and the absorbed dose rate of the irradiated water. Even with the detailed estimation of decay heat as summarized in Section 4.1, the absorbed dose rate of pool water due to γ-irradiation through the decay heat of spent fuel depends greatly on fuel management. In some practices, spent fuel is stored (a) in locations which provide the largest criticality safety margin and in other cases (b) with longer cooled fuel relocated to secure positions for the new batch of incoming high decay-heat spent fuel. Due to the shielding effects of the spent fuel from previous cycles, case (a) results in a lower absorbed dose rate on average but the volume of irradiated water increases.

(2) Total volume of irradiated water
The total number of spent fuel assemblies in the 1F4 SFP was 1331 (i.e., the evacuated core load of 548 bundles plus 685 bundles from previous cycles) at the time of the accident. In the new calculation, all of the spent fuel was assumed to have been shuffled (i.e., mixed together) and stored in 22.2 standard spent fuel racks which measured 1.2 m in width, 1.7 m in length and 4.2 m in depth. The total volume of irradiated water is assumed to be 166 m^3, which is equal to the total volume of water contained in the spent fuel racks considering the linear absorption coefficient of γ-ray, which extends beyond the (neutron) *effective height* (i.e., 3.66 m).

(3) Recycling of the irradiated water
After irradiation of the water flowing through the fuel channels, it should contain different concentrations of stable molecular species (i.e., H_2, O_2 and H_2O_2) compared with the inlet concentrations. After being ejected from the spent fuel assemblies, these molecular species should be mixed with the bulk of the pool water and a portion should return to the fuel bundles with the high decay heat. Through modeling studies, the author found that the dilution and recycling process significantly affect the hydrogen generation rate. In the best estimate calculation as covered in Section 4.2.5, the author will provide a case with optimal mixing in the bulk of pool water.

4.2.2. Update of previous estimation

Since TEPCO's official scenario is not convincing, the author investigated the possibility of hydrogen generation through RIE in Unit 4. The author first anticipated that the RIE mechanism may not be involved in the hydrogen explosion event in 1F4 SFP. It is because hydrogen generation levels off with time in the reactor core when the reactor water temperature is unchanged in 1F1–1F3 (Saji, 2014a,b). This phenomena was found due to a rapid decrease in decay heat and an increase in DH which further suppresses the radiological decomposition of water. Nevertheless a potential hydrogen generation was investigated when the forced pool water-cooling was terminated due to SBO and a gradual water temperature increase occurred until it resulted in the hydrogen explosion.

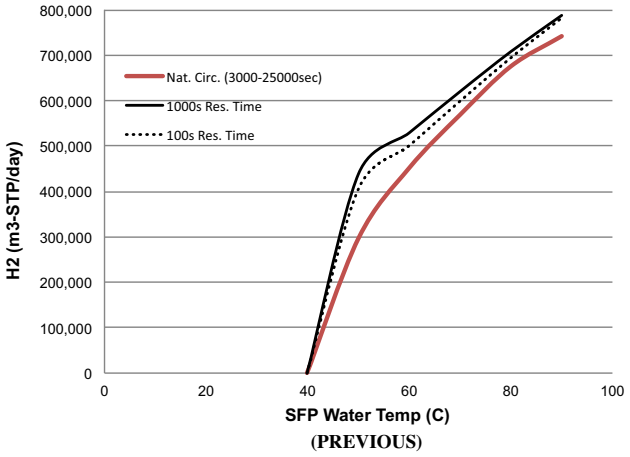

Fig. 7. H_2 gas generation in Unit 4 SFP (m^3-STP/day).

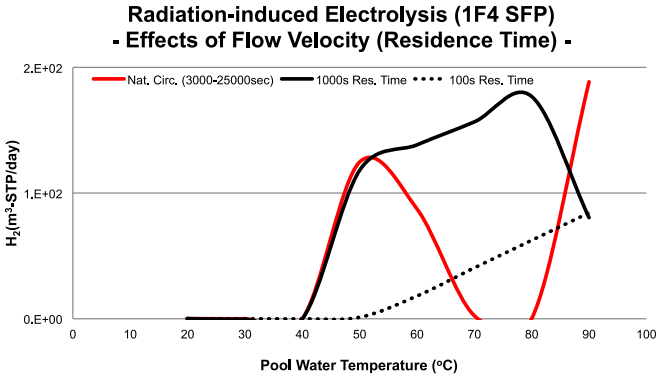

Fig. 8. H_2 gas generation in Unit 4 SFP (m^3-STP/day).

These observations lead the author to search for a potential mechanism by changing the pool water temperature and flow velocity in the spent fuel. During the trial calculations it was discovered accidentally that SBO induced a rapid initiation of electrolysis when the pool water temperature exceeded 40 °C. The verification as presented in this paper revealed that an error had slipped in the previous analysis (Saji, 2014b) while converting the *G*-values in a conventional unit into an SI unit, thereby resulting in an overestimation of the hydrogen generation and over simplification related to the effects of flow rates.

The previous results are included in Fig. 7 and the updated results are shown in Fig. 8. The estimated hydrogen generation rates increases drastically when the pool water temperature exceeds 40 °C in both cases with the residence time (i.e. $1/\dot{\nu}$ of Eq. (9)) of 1000 s whereas this surge is not as prominent in the forced convection region of 100 s in the updated results (Fig. 8).

The plant data used for these two calculations are unchanged, although the absorbed dose rate was 3 orders of magnitude smaller in the updated calculation. Fig. 8 reveals that the actual behavior of the RIE is complicated due to the flow velocity effect that induced serious changes in the radiation chemical material balance.

When the coolant flow rate is in the single-phase natural convection regime, the hydrogen generation rate decreases after surpassing 50 °C. This strange behavior is found to be due to a delicate balance between the hydrogen and oxygen concentrations as shown in Fig. 9. These two concentrations appear as mirror images of each other. A large amount of both the hydrogen and oxygen

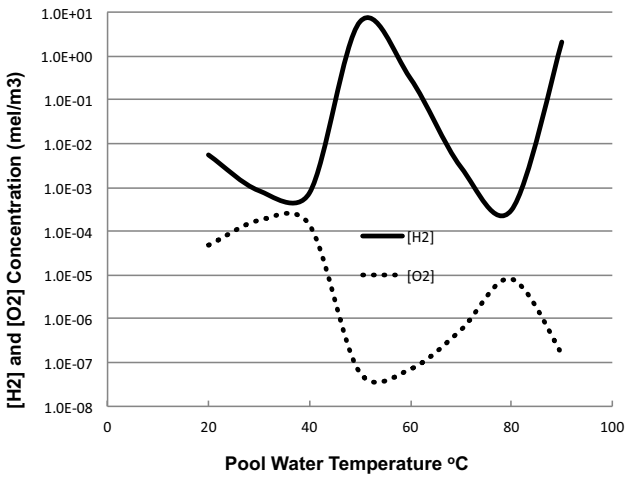

Fig. 9. Variation of H_2 and O_2 concentration of the irradiated water with respect to pool water temperature.

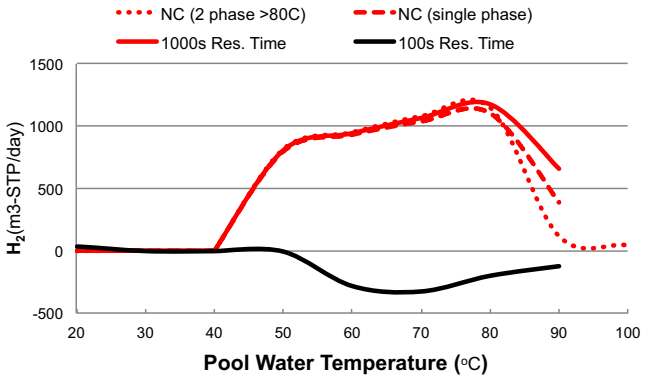

Fig. 10. H_2 gas generation in Unit 4 SFP (m^3-STP/day).

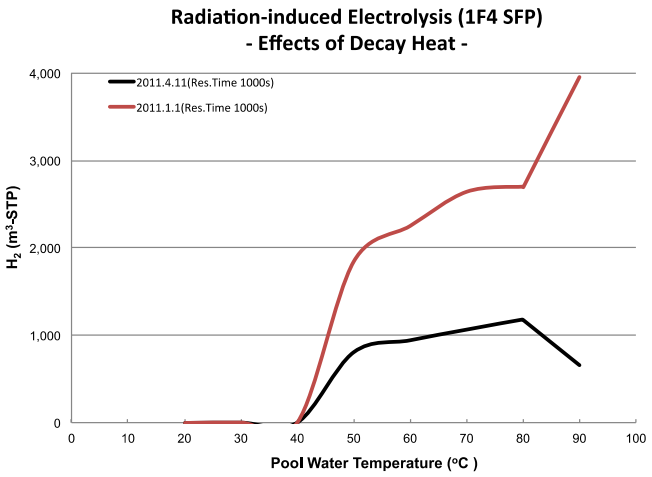

Fig. 11. H_2 gas generation in Unit 4 SFP (m^3-STP/d).

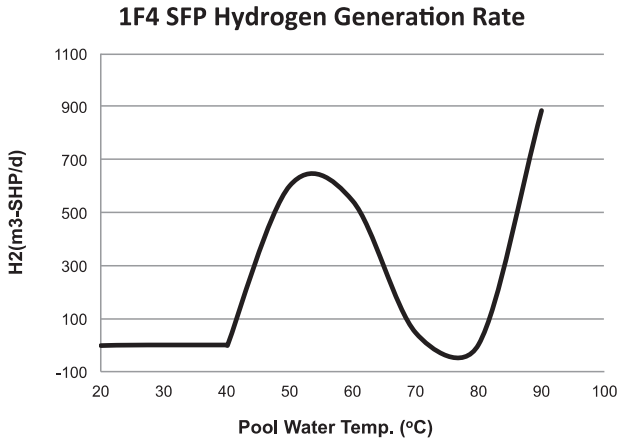

Fig. 12. Best estimate H_2 gas generation in Unit 4 SFP.

gases are generated when the pool water temperature exceeds 40 °C. This configuration behaves as an "oxygen generator" between 70 and 80 °C with a natural circulation cooling, as shown in Fig. 9.

4.2.3. Effects of spent fuel management in SFP

Fig. 10 demonstrates another update where the spent fuel with high decay heat was shuffled in the SFP using 22 racks (whereas Fig. 8 describes a situation where the evacuated core inventory was localized by using 9 adjacent racks). The volume of the irradiated water was 166 m^3 in the new calculation whereas it was 50 m^3 in Fig. 8. A single-phase as well as sub-cooled boiling natural circulation is assumed in Fig. 10 although the differences are not substantial.

When the residence time is 100 s, the electrical current is flowing in a negative direction above 50 °C which indicates the reverse reaction as defined in Eq. (3) from the spent fuel with high decay heat and hydrogen generation in the spent fuel from previous cycles. The complex results of hydrogen generation calls for the development of a "safety map" although the author hesitates providing one at this time due to the lack of experimental data to verify this hypothesis. Experimental data of the electrical current flowing between the anodic- and cathodic region is highly awaited for further verification.

4.2.4. Higher decay heat effects – a safety margin

Since the error introduced through the absorbed dose rate resulted in a significant difference in the rate of hydrogen production, a verification calculation was created to identify a safety margin by changing the decay heat. Fig. 11 indicates the results for two cases where the SBO actually occurred on March 11, 2011 in the first case whereas an arbitrary hypothetical case assumed to occurred on January 1, 2011. In the second case, the core evacuation was assumed to be completed one month after the reactor shutdown. The decay heat in this case is approximately 3 times larger than the first case. The sudden bends in both curves at 80 °C are due to the introduction of sub-cooled boiling at this temperature.

Note that the hydrogen generation rates increase substantially with higher decay heat, approaching the shapes shown in Fig. 7.

4.2.5. Best estimation for the Fukushima Daiichi Unit 4

After reviewing all of these modeling studies, the author provides the best estimation of the hydrogen generation rate with the following parameters.

(1) Decay heat of the fuel bundles in the cathode: as introduced in Table 2, the decay heat of fuels from 24th and 23rd cycles represent the dominant decay heat fuel bundles. The corresponding total decay heat is 1.83 MWt with the irradiated water volume of 80.7 m^3. The corresponding "dilution factor" was 0.09 in the case of perfect mixing with the bulk of the pool water.
(2) Natural convection modeling: the single phase natural convection followed with sub-cooled boiling heat transfer above 80 °C.

Other parameters follow Section 3.4 with the adaptation of the 1F4 SFP configuration. The results are illustrated in Fig. 12. It should

be noted that the hydrogen generation results from a very complicated material balance through radiation- and electro-chemical processes. Some of the key factors of the processes include:

- Absorbed dose rate and volume of irradiated water
- Velocity (i.e., "residence time") of the water in irradiation and some mechanism of the irradiated water recirculation
- Some mechanism of electrons transport between cathodic- and anodic regions (i.e., "long-cell action").
- Some mechanism (e.g., depressurization through SRVs) to prevent accumulation of generated hydrogen.

5. Conclusions

Since the scientific cause for a series of hydrogen explosions during the Fukushima accident has not been established, this phenomenon was first widely reviewed during normal operations to severe accidents by performing scoping estimations.

Since the amount of hydrogen release is suppressed due to reverse reactions of the radiation chemical process, it is unlikely that the so-called water radiolysis is the root cause of the hydrogen explosion at Fukushima.

5.1. Hydrogen generation upon SBO in 1F1–1F3

The author finally tested a new mechanism, "radiation-induced electrolysis," which has been applied to his corrosion studies for the past several years. His theory has been verified with the published in-pile test data of potential differences, although he has never tried to apply it to a severe accident study. This theory enables one to estimate the hydrogen generation rate upon SBO prior to the potential core disruption and melting where a zirconium-steam reaction may be significant.

The results predict that the total inventory of hydrogen gas inside the RPV may reach as much as 10,000 m^3-STP in just half a day during the SBO due to a high decay heat soon after the reactor trip. Therefore, in the event of a SBO the early safe disposal of accumulated hydrogen gas is indispensable in parallel with emergency reactor cooling for boiling water reactors without hydrogen dosing to suppress water radiolysis.

5.2. Hydrogen generation in 1F4 SFP

The author searched for a potential radiation chemical mechanism for the hydrogen explosion in Unit 4 of the Fukushima Daiichi during the accident by changing the pool water temperature and flow velocity of the spent fuel. During the trial calculations SBO was found to have induced a rapid initiation of electrolysis when the pool water temperature reached approximately 40 °C.

The present estimation of the hydrogen generation rate is still large enough to have induced the explosion in 1F4 SFP since as large as 1000 Nm^3/d is estimated when the pool water temperature exceeds approximately 40 °C. It also revealed that the behavior of radiation chemical process is much more complicated than simply the dependence on temperature. It depends on the management of spent fuels in the SFP, absorbed dose rate and volume of irradiated- and mixing volume of water as well as its flow velocity (i.e., residence time of the water staying in the highly active region of spent fuel).

In order to abide to these complexities the author proposes the simple solution of inserting a ceramic insulator to prevent direct metallic contact of the spent fuel racks to the SFP liner thereby disconnecting the flow of electrons from the anodic cooled fuel assemblies.

However the author has reservations regarding the current results as our knowledge is extremely limited as to the chemical characteristics of the cooling water in the core region. In particular the application of the author's basic approach for his corrosion study to the severe accident situation has been established essentially without experimental data to verify. However the observed phenomenology of a series of hydrogen explosions during the Fukushima accident is not contradictory to the author's prediction.

Obviously understanding the phenomena occurring through radiation-induced electrolysis in the Fukushima accident is not complete, and the theoretical framework of radiation chemistry applicable to severe accidents in LWRs has to be more firmly established.

Appendix A. A fact sheet of HAMAOKA UNIT 1 accident

This appendix summarizes the hydrogen-explosion/pipe-rupture accident which occurred at the Hamaoka Unit 1 in a "fact sheet" style (Fig. A1).

- Hamaoka Unit 1: 540 MWe, BWR.
- Occurred: 17:02 on November 7th, 2001.
- Pant state: steady state of operation during a scheduled ECCS test for manual start up of HPCI pump.
- Water chemistry: hydrogen water chemistry, supplemented with noble metal^{TM} water chemistry.
- Operators' observation: blast noise observed by the operators of the central control room as well as at local panels.
- Trip sequence: HPCI trip followed with containment isolation.
- Environmental monitoring: 30–40 nGy/h (no change).
- Confirmation: a maintenance crew accidentally went inside the reactor building, 17:20 and identified that the 1F and 2F floors were wet with water. The fire alarms were triggered due to steam leakage.
- Causes of the explosion: hydrogen burn induced from hydrogen gas accumulated at the top portion of the Steam Condensate piping system. The hydrogen was transported with steam which condensed in this dead end pipe thereby releasing hydrogen gas.
- Hydrogen concentration: 0.6% volume in the similar riser pipe location of RHRS A and 19% of O_2 gas. Similarly in Unit 2 RHRS A, H_2 = 46%, O_2 = 23%: RHRS B, H_2 = 27%, O_2 = 23%.
- Estimated hydrogen accumulation after 8 months of operation: 6–8 meter from the condensed water surface, with H_2 = 66% and O_2 = 33%, N_2 = 1%.
- Causes of ignition: in spite of the follow-up experiments, the causes of ignition were not clarified however it is suspected to have been induced by minuscule particles of noble metal deposited on the surface of the piping.

Fig. A1. Pipe rupture at the steam condensate system of RHRS (pipe size: OD = 165 m/m, WT = 11 m/m).

- Ignition tests: self-ignition at 340–370 °C, 5–8 MP with dry mixture of hydrogen and oxygen. No self-ignition with steam. Some cases of self-ignition with a noble-metal catalysis.
- Combustion to detonation transition: At 1–2 m from the ignition point.
- Maximum plastic deformation of pipes: greater than 23%.
- Estimated leakage: approximately 2 tons of steam. The estimated radioactive leakage was 8×10^8 Bq.
- Brunsbüttel accident: a similar pipe rupture incident occurred on December 14, 2001 at the Brunsbüttel NPP in Germany.

References

ANS-5.1, 1973, October. Decay Energy Release Rates Following Shutdown of Uranium-Fueled Thermal Reactors, Draft ANS-5.1/N18.6.

Brunsbüttel reactor, 2002. http://www10.antenna.nl/wise/index.html?http://www10.antenna.nl/wise/564/5379.html.

Caër, S.L., 2011. Water radiolysis: influence of oxide surfaces on H_2 production under ionizing radiation. Water 3, 235–253, http://dx.doi.org/10.3390/w3010235 www.mdpi.com/journal/water.

Elliot, A.J., Bartels, S.M., 2009. The Reaction Set, Rate Constants and *G*-values for the Simulation of the Radiolysis of Light Water over the Range 20 to 350 °C Based on Information Available in 2008. AECL 153-127160-450-001.

Farrow, L.A., Edelson, E., 1974. The steady state approximation: fact or fiction? Int. J. Chem. Kinet. 6, 787–800.

Investigation Committee, 2012. On the Accident at the Fukushima Nuclear Power Stations, 2012. http://www.icanps.go.jp/eng/.

Jay, I.O., et al., 1995. Improved QSSA methods for atmospheric chemistry integration. In: Report on computational mathematics, No. 67/1995. Dept. of Math., Univ. of Iowa http://www.siam.org/journals/sisc/18-1/28303.html.

Kysela, J., et al., 2001. Corrosion Potential Dependence on Oxygen, Hydrogen and Hydrogen Peroxide in Reactor Water Loop at BWR Conditions. Water Chemistry of Nuclear Reactor Systems 8, BNES.

McMaster Nuclear Reactor, 1998. Technical Report 1998-03. McMaster University.

Maruyama, S., 2015. Validation of behavior of isolation condenser (IC) during accident at Fukushima Daiichi NPP nuclear power plant, Unit 1 – And yet, the IC was working after the tsunami arrival. In: Proc. of ICONE-23, May 17-21, Chiba, Japan, Nagoya Univ. http://www.nagoya-u.ac.jp/about-nu/public-relations/researchinfo/upload_images/20150320_esi.pdf#search.

Naito, M., et al., 2003a. Analysis on pipe rupture of steam condensation line at Hamaoka-1, (I) accumulation of non-condensable gas in a pipe. J. Nucl. Sci. Technol. 40 (December (12)), 1041–1051.

Naito, M., et al., 2003b. Analysis on pipe rupture of steam condensation line at Hamaoka-1, (II) hydrogen combustion and pipe deformation. J. Nucl. Sci. Technol. 40 (December (12)), 1041–1051.

National Diet of Japan, 2012. Fukushima Nuclear Accident Independent Investigation Commission, 2012. http://warp.da.ndl.go.jp/info:ndljp/pid/3856371/naiic.go.jp/en/index.html.

Nuclear Emergency Response Headquarters, 2011, June. Report of Japanese Government to the IAEA Ministerial Conference on Nuclear Safety – The Accident at TEPCO's Fukushima Nuclear Power Stations.

Nuclear Emergency Response Headquarters, 2011, September. Additional Report of the Japanese Government to the IAEA – The accident at TEPCO's Fukushima Nuclear Power Stations.

Nuclear and Industrial Safety Agency, 2002. Investigation Report on Pipe Rupture Incident at Hamaoka Nuclear Power Station Unit-1 (English Version), July 2002. Nuclear and Industrial Safety Agency, Ministry of Economy, Trade and Industry, Tokyo, Japan.

Saji, G., 2010a. Radiation induced 'long cell' (macro-cell) corrosion in light water reactors. Nucl. Eng. Des. 240, 1340–1354.

Saji, G., 2010b. Chemico-physical causes of long-cell action corrosion in light water reactors, ICONE18-29714. In: 18th Int. Conf. on Nuc. Eng., Xi'an, China.

Saji, G., 2013a. Scientific bases of water chemistry for corrosion control of NPPs by integration of radiation- and electro-chemistry, ICONE21-16525. In: 21st Int. Conf. on Nucl. Eng., Chengdu, China.

Saji, G., 2013b. Chemico-physical causes of radiation-induced "long-cell" action corrosion in water-cooled reactors. Nucl. Eng., 102–116, http://dx.doi.org/10.1016/j.nucengdes.2012.12.006.

Saji, G., 2014a. Review on Water Radiolysis in the Fukushima Daiichi Accident – Potential Cause Of Hydrogen Generation And Explosion – ICONE22-0991.

Saji, G., 2014b. "Radiation-Induced Electrolysis", A Potential Root Cause of Hydrogen Explosions in the Fukushima Daiichi Accident – NPC 2014 Supporo (Submission #10213).

Saji, G., 2014c. Characterization of in-core water chemistry for corrosion control of LWRs, ICONE22-30990. In: 22nd Int. Conf. on Nucl. Eng., Prague, Czech Republic.

Saji, G., 2015. "Radiation-induced electrolysis (iii)" – a potential root cause of hydrogen explosions in the Fukushima Daiichi accident, ICONE23-1093. In: Proc. of 23rd Int. Conf. on Nucl. Eng., May 17–21, Chiba, Japan.

Saji, G., 2016a. Radiation-induced electrolytic corrosion of LWRs (Part 1): Basic mechanism and implications in degradation phenomena. ICONE24-60894. In: Proceedings of 24th Int. Conf. of Nuc. Eng., Charlotte, NC, USA.

Saji, G., 2016b. Radiation-induced electrolytic corrosion of LWRs (Part 2): Verification of in- and out-core redox potential differences. ICONE24-60895. In: Proceedings of 24th Int. Conf. of Nuc. Eng., Charlotte, NC, USA.

Sander, R., 1999. Compilation of Henry's Law Constants for Inorganic and Organic Species of Potential Importance in Environmental Chemistry, Version 3 (April 8, 1999). http://www.mpch-mainz.mpg.de/~sander/res/henry.html.

Spinks, J.W.T., Woods, R.J., 1990. An Introduction to Radiation Chemistry. P252, 3rd ed. John Wiley and Sons.

Takiguchi, H., Sekiguchi, M., Christensen, H., Flygare, J., Molander, A., Ullberg, M., 2000. In-pile loop experiment and model calculations for radiolysis of PWR primary coolant. In: Conf. Water Chem. of Nucl. Reactor Sys. 8, BNES, Bournemouth.

Takiguchi, H., Ullberg, M., Uchida, S., 2004. Optimization of dissolved hydrogen concentration for control of primary coolant radiolysis in pressurized water reactors. J. Nucl. Sci. Technol. 41 (5), 6-1–6-9.

TEPCO, 2012. Investigation Report of the Fukushima Nuclear Accident (in Japanese). http://www.tepco.co.jp/en/press/corp-com/release/2012/1205638_1870.htm.

TEPCO website, 2003: http://www.tepco.co.jp/cc/press/03082103-j.html.

TEPCO's website, 2014: http://www.tepco.co.jp/nu/fukushima-np/handouts/2014/images/handouts_141031_12-j.pdf.

TEPCO's website, 2015a: http://www.tepco.co.jp/en/nu/fukushima-np/handouts/2015/images/handouts_150319_01-e.pdf.

TEPCO's website, 2015b: http://www.tepco.co.jp/en/nu/fukushima-np/handouts/2015/images/handouts_150417_01-e.pdf.

Zmikto, M., 2003, December. Materials and Water Chemistry Research in the Research Reactor Test Facilities at NRI Rez. Presented at a lecture given at Tohoku University, Sendai, Japan.